Experimental Lab Report - Compton Scattering

Ruaidhrí Campion
19333850
SF Theoretical Physics

December 2020

Contents

1 Abstract

In this experiment, Compton's expression for the energy of a scattered photon was verified. The Compton energy of a quasi-free electron was found to be 528.88758 ± 8.97132 keV. The energy of the incident Caesium source was found to be 658.66801 ± 6.22727 keV. The forwards and backwards Compton edges were estimated to be 186.94926 ± 1.16953 keV and 475.78062 ± 1.58248 keV, corresponding to a scattering angle range of $\frac{\pi}{4}$ rad to π rad.

2 Introduction

In 1923, Arthur Compton was experimenting in Washington University when he observed that, after scattering an electron using a photon, the wavelength of the incident photon changed.[1] Today, this phenomenon is known as the Compton effect. This discovery was vital in the development of the wave-particle duality, as it conclusively proved that light cannot be described purely as a wave.[2] The derivation of the Compton scattering formula is as follows.

A photon of energy E_0 and wavelength λ_0 strikes an electron of mass m_e^* at rest with rest energy E_1. The photon deflects an angle θ and has energy E and wavelength λ after the collision. The electron deflects an angle φ and has energy E_2 and momentum p_2 after the collision.

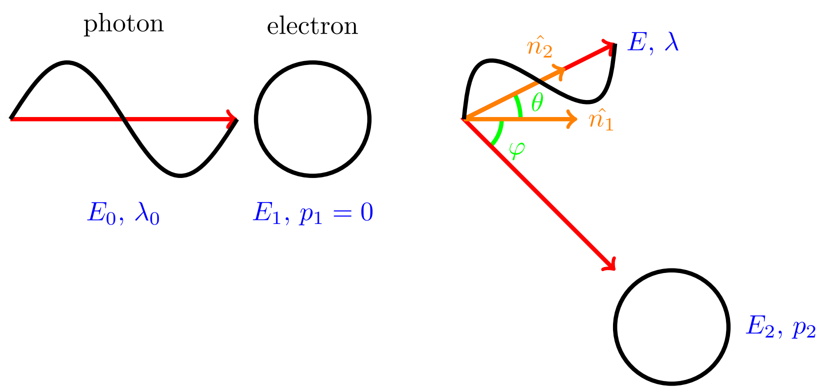

Figure (a): Diagram showing Compton scattering of a photon and electron

$$\text{Energy conservation} \implies E_0 + E_1 = E + E_2$$
$$E_2 = E_0 - E + m_e^* c^2 \quad (1)$$

[1]Compton, 1923
[2]Griffiths, 1987

$$\text{Momentum conservation} \implies \frac{E_0}{c}\hat{n}_1 = \frac{E}{c}\hat{n}_2 + \vec{p}_2$$
$$\vec{p}_2 \cdot \vec{p}_2 = \frac{1}{c}(E_0\hat{n}_1 - E\hat{n}_2) \cdot \frac{1}{c}(E_0\hat{n}_1 - E\hat{n}_2)$$
$$p_2^2 = \frac{1}{c^2}(E_0^2 - 2E_0E\cos\theta + E^2) \tag{2}$$

$$\text{Energy-momentum invariant} \implies E_i^2 - p_i^2c^2 = (m_e^*)_i^2\, c^4 \tag{3}$$

$$E\,(\lambda_i) \equiv \frac{hc}{\lambda_i} \tag{4}$$

Using equations (1), (2) & (3),

$$\begin{aligned}
(m_e^*)^2\, c^4 &= (E_0 - E + m_e^*c^2)^2 - \frac{c^2}{c^2}(E_0^2 - 2E_0E\cos\theta + E^2) \\
(m_e^*)^2\, c^4 &= E_0^2 - 2E_0E + E^2 + 2m_e^*c^2(E_0 - E) + (m_e^*)^2\, c^4 \\
&\quad - E_0^2 + 2E_0E\cos\theta - E^2 \\
0 &= -2E_0E + 2m_e^*c^2(E_0 - E) + 2E_0E\cos\theta \\
2(E_0 - E)m_e^*c^2 &= 2E_0E(1 - \cos\theta) \\
\frac{E_0 - E}{E_0E} &= \frac{1 - \cos\theta}{m_e^*c^2} \\
\frac{1}{E} - \frac{1}{E_0} &= \frac{1 - \cos\theta}{m_e^*c^2} \qquad (5) \\
(4) \implies \frac{\lambda}{hc} - \frac{\lambda_0}{hc} &= \frac{1 - \cos\theta}{m_e^*c^2} \\
\lambda\,(\lambda_0, \theta) &= \lambda_0 + \frac{h\,(1 - \cos\theta)}{m_e^*c} \qquad (6) \\
&= \lambda_0 + \lambda_C\,(1 - \cos\theta)\,, \qquad (7)
\end{aligned}$$

where $\lambda_C = \frac{h}{m_e^*c}$ is the Compton wavelength of an electron of effective mass m_e^*.

If it assumed that the electron is free, i.e. $m_e^* \cong m_e$, the value of λ_C can be determined.

$$\begin{aligned}
\lambda_C &\equiv \frac{h}{m_e^*c} \\
&= \frac{6.6260693 \times 10^{-34}}{9.1093826 \times 10^{-31} \cdot 2.99792458 \times 10^{8}} \\
&= 2.42631022 \times 10^{-12} \\
&\approx 2.426 \text{ pm}
\end{aligned}$$

The energy E_C corresponding to this value can also be determined.

$$
\begin{aligned}
(4) \implies E\left(\lambda_C\right) &= \frac{hc}{\lambda_C} \\
&= \frac{6.6260693 \times 10^{-34} \cdot 2.99792458 \times 10^{8}}{2.42631022 \times 10^{-12}} \\
&= 8.18710479 \times 10^{-4} \text{ J} \\
&= 5.10998921 \times 10^{5} \text{ eV} \\
&\approx 511 \text{ keV}
\end{aligned}
$$

Einstein's mass-energy equivalence relation[3] for the energy of the electron can also be deduced.

$$
\begin{aligned}
(4) \implies E_C &= \frac{hc}{\lambda_C} \\
\lambda_C &\equiv \frac{h}{m_e^* c} \\
\implies E_C &= \frac{hc}{\frac{h}{m_e^* c}} \\
&= m_e^* c^2
\end{aligned}
$$

The Klein-Nishina expression was derived by Oskar Klein and Yoshio Nishina in 1928, and gives the differential scattering cross section σ as a function of E and θ.[4]

$$
\sigma\left(E, \theta\right) = r_0^2 \frac{1 + \cos^2\theta}{2} \frac{1}{\left(1 + \frac{E}{E_C}\left(1 - \cos\theta\right)\right)^2} \left(\frac{\left(\frac{E}{E_C}\right)^2 \left(1 + \cos\theta\right)^2}{\left(1 + \cos^2\theta\right)\left(1 + \frac{E}{E_C}\left(1 - \cos\theta\right)\right)} + 1 \right) \tag{8}
$$

In this experiment, photons were scattered by a scattering target and detected by a scintillator. The scattering angle was varied and the energy of the scattered photon changed as a result.

[3] Einstein, 1905

[4] Klein, Nishina, 1928

3 Experimental Method

1. Install the ${}^{241}_{95}Am_{146}/{}^{137}_{55}Cs_{82}$ mixed calibration source in the collimator arrangement. Measure the energy spectrum for approximately 15-30 minutes. Ensure that the number of channels used for each spectrum remains the same throughout the experiment.

2. Remove the calibration source. Place the aluminium scattering target in the centre of the apparatus, and set up the ${}^{137}_{55}Cs_{82}$ main source so that it points at the scattering target.

3. For various scattering angles θ, measure the energy spectrum produced by the scattered photons, again for approximately 15-30 minutes per angle.

4. Using the mixed calibration table (Table (i), Results section), locate the peaks of the calibration energy spectrum and plot a linear calibration curve of energy against channel number, and find the corresponding equation.

5. For each scattering energy spectrum, locate the peak corresponding to the scattered photon. Using the calibration curve equation, calculate the energy of the scattered photon E.

6. Using the calculated data from step 5, plot E against θ, with equation (5) as the fitting curve. From this plot, deduce the values of E_0 and E_C.

7. Estimate the energy of the Compton edges by locating the asymmetric peaks on the calibration energy spectrum.

8. Using the actual values for E_0 and E_C in equations (5) and (8), plot the differential scattering cross section σ as a function of θ.

4 Results

Due to the large number of figures, Figures (b)-(q) used in this section are in the Appendix section at the end of the report.

Table (i):[5] Mixed preparation calibration table for ${}^{241}_{95}Am_{146}/{}^{137}_{55}Cs_{82}$.

E, keV	ΔE, keV	Identification
18	4	Am X-ray
32	2	Cs X-ray
59.54	0.01	Am gamma
75	1	Pb X-ray
662	1	Cs gamma

Three distinct peaks were located on the graph of the calibration energy spectrum (Figure (b), page 10) and identified as Cs X-ray, Pb X-ray and Cs gamma, using Table (i). Voigt fits were used to find the channel number for each peak (Figures (c)-(e), pages 11-12).

Table (ii): Energy and corresponding channel number obtained from calibration energy spectrum.

Energy, keV	Channel Number
32 ± 2	19.91987 ± 0.15867
75 ± 1	48.56729 ± 0.06400
662 ± 1	463.54768 ± 0.04682

This data was plotted (Figure (f), page 12), and the calibration equation was found to be

$$\text{Energy} = (1.41584 \pm 0.00348) \times \text{Channel Number} + (5.72174 \pm 1.08138)\,. \quad (9)$$

For the Compton scattering, energy spectra were plotted for scattering angles $\theta = 0, \frac{\pi}{3}, \frac{\pi}{2}, \frac{2\pi}{3}, \frac{3\pi}{4}$ and $\frac{5\pi}{6}$ rad, and the location of each corresponding peak was found using Voigt fitting (Figures (g)-(l), pages 13-18).

The following data was obtained from these plots using equation (9), and the graph of $E(\theta)$ was plotted using equation (5) (Figure (m), page 19).

Table (iii): Positions of energy peaks corresponding to each scattering angle.

θ, rad	Channel Number	E, keV
$0 \pm \frac{\pi}{36}$	462.28911 ± 0.11878	660.24915 ± 1.94571
$\frac{\pi}{3} \pm \frac{\pi}{36}$	286.14333 ± 1.90173	410.85491 ± 3.06770
$\frac{\pi}{2} \pm \frac{\pi}{36}$	198.33481 ± 1.11816	286.53210 ± 2.03767
$\frac{2\pi}{3} \pm \frac{\pi}{36}$	158.75529 ± 0.62938	230.49383 ± 1.50620
$\frac{3\pi}{4} \pm \frac{\pi}{36}$	146.70101 ± 0.50565	213.42690 ± 1.39376
$\frac{5\pi}{6} \pm \frac{\pi}{36}$	140.26828 ± 0.31305	$204.31918 \pm 1.26653^{*}$

[5] TCD School of Physics, 2020

E_0 and E_C were estimated from Figure (m) to be 658.66801 ± 6.22727 keV and 528.88758 ± 8.97132 keV, respectively.

Figure (n) (page 20) is a graph showing the variance between the experimentally calculated dependence of E on θ and the theoretical curve.

Using the calibration energy spectrum, the Compton edges were estimated to be 186.94926 ± 1.16953 keV and 475.78062 ± 1.58248 keV (Figure (o), page 20).

Figure (p) (page 21) is a plot of the differential scattering cross section σ against θ, using equation (8).

Figure (q) (page 21) is a rough simulation of the energy spectrum using the following data obtained throughout the experiment.

Table (iv): Coordinates of rough simulation of energy spectrum.

E, keV	Iterations (arbitrary)
0	0
18 ± 4	2
25	1
32 ± 2	1.5
39	1
59.54 ± 0.01	4.6
67.27	1.9
75 ± 1	2.5
100	0.5
170	0.35
186.94926 ± 1.16953	1
475.78062 ± 1.58248	0.5
500	0.1
600	0.1
662 ± 1	5
724	0.1

5 Discussion

Thick lead bricks were used in this experiment as a makeshift tunnel to ensure that radiation from exterior sources were minimised.

The channel number range used in this experiment was 0-511, and so the energy range covered was (5.72174 ± 1.08138)-(729.21598 ± 2.08126) keV.

Figures (m) and (n) verify Compton's expression (equation (5)), within experimental error. The deduced values for E_0 and E_C of 658.66801 ± 6.22727 keV and 528.88758 ± 8.97132 keV are relatively close to the actual values of 661.657 keV and 5.110 keV, respectively.

Using the deduced value for E_C, the effective electron mass m_e^* in Al was found to be approximately $(9.4282769 \pm 0.1599283) \times 10^{-31}$ kg, which agrees with the approximation of $m_e^* \approx m_e = 9.1093826 \times 10^{-31}$ kg.

The Compton edges were estimated to be 186.94926 ± 1.16953 keV and 475.78062 ± 1.58248 keV. Within experimental error, this agrees with the theoretical values of 184 keV and 478 keV.[5] Using equation (5), these energies correspond to scattering angles of approximately π rad and $\frac{\pi}{4}$ rad, respectively, which suggests that Compton scattering would only be detected by the detector between $\frac{\pi}{4}$ rad and π rad. Energy spectra were obtained for $\theta = \frac{\pi}{6}$ and $\theta = \frac{\pi}{4}$, however were omitted from the Results section due to indistinguishable peaks. This lines up with the suggestion of the Compton scattering range of $\frac{\pi}{4}$ rad to π rad.

The graph of the differential scattering cross section σ against scattering angle θ is roughly linear from 0 rad to $\frac{\pi}{4}$ rad, and then asymptotes to near 0 from $\frac{\pi}{4}$ rad to π rad.

6 Error Analysis

The uncertainty in the scattering angle θ was taken to be a constant 5° or $\frac{\pi}{36}$ rad.

All uncertainties shown on graphs were propagated automatically by Origin.

All other uncertainties were calculated using the formula

$$\Delta f = \sqrt{\sum_{i=1}^{n} \left(\frac{\partial f}{\partial x_i} \Delta x_i \right)^2}$$

$$\text{where } f = f(x_1, x_2, \ldots, x_n)$$

$$\Delta x_i \equiv \text{uncertainty in } x_i$$

*For example, the uncertainty in the energy of the scattered photon E was calculated as follows.

$$\begin{aligned}
\text{Channel Number} &= 140.26828 \\
\Delta\,(\text{Channel Number}) &= 1.26653 \\
E &= mx + c \\
&= 1.41584 \times 140.26828 + 5.72174 \\
&= 204.31918 \\
\Delta E &= \sqrt{\left(\frac{\partial E}{\partial m}\Delta m\right)^2 + \left(\frac{\partial E}{\partial x}\Delta x\right)^2 + \left(\frac{\partial E}{\partial c}\Delta c\right)^2} \\
&= \sqrt{(x\Delta m)^2 + (m\Delta x)^2 + (\Delta c)^2} \\
&= \sqrt{(\text{Channel Number} \times 0.00348)^2 + (1.41584 \times \Delta(\text{Channel Number}))^2 + 1.08138^2} \\
&= 1.26653 \\
\implies E &= 204.31918 \pm 1.26653 \text{ keV}
\end{aligned}$$

7 Conclusion

Compton's expression for the energy of a scattered photon was verified. Calculated values for E_C, E_0 and m_e^* were found to agree with their real values, within experimental error. The Compton edges were estimated and agreed with the allowed range of scattering angles.

8 References

1: A. Compton, *Physical Review*, vol. 21, iss. 5, pp. 483-502, 1923.

2: D. Griffiths, *Introduction to Elementary Particles*, Wiley, Hoboken, 1987.

3: A. Einstein, *Annalen der Physik*, vol. 323, iss. 13, pp. 639–641, 1905.

4: O. Klein, Y. Nishina, *Zeitschrift für Physik*, vol. 52, pp. 853-868, 1929.

5: TCD School of Physics, provided experiment description, 2020

All figures are of my own making, using either TikZ, Origin or Mathematica.

9 Appendix

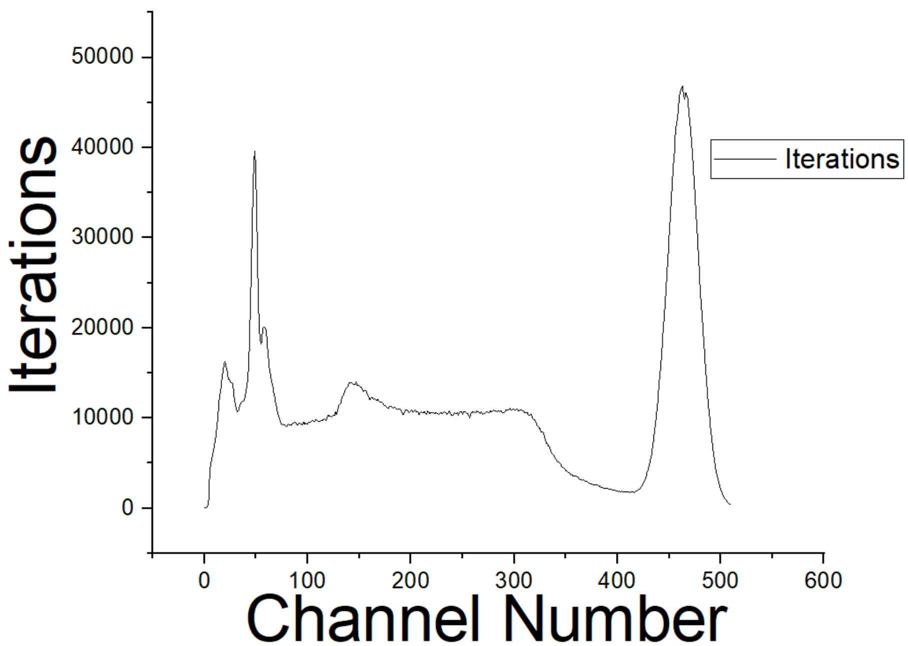

Figure (b): Energy spectrum of calibration source. Data collected for 3,805 seconds. Notable peaks: Cs X-ray, Pb X-ray, Cs gamma.

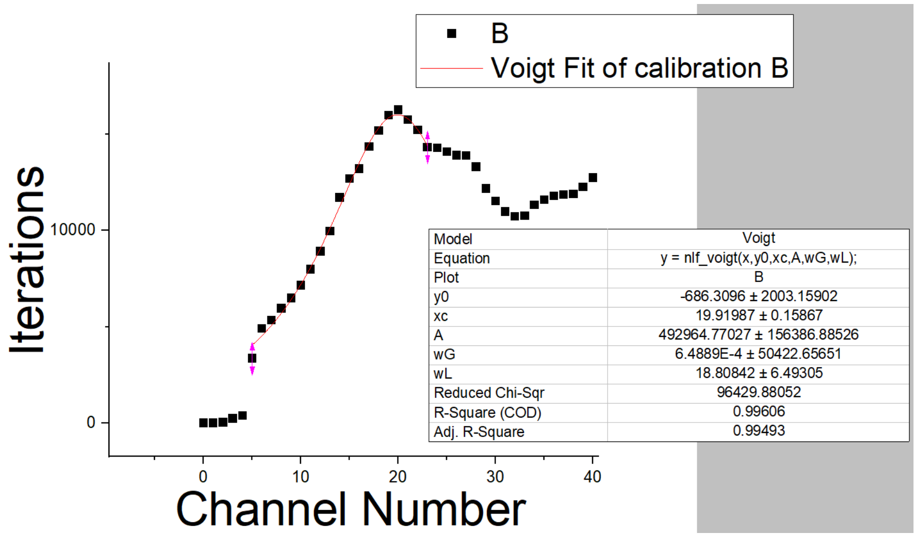

Figure (c): Voigt fit of Cs X-ray peak, corresponding to a channel number of 19.91987 ± 0.15867.

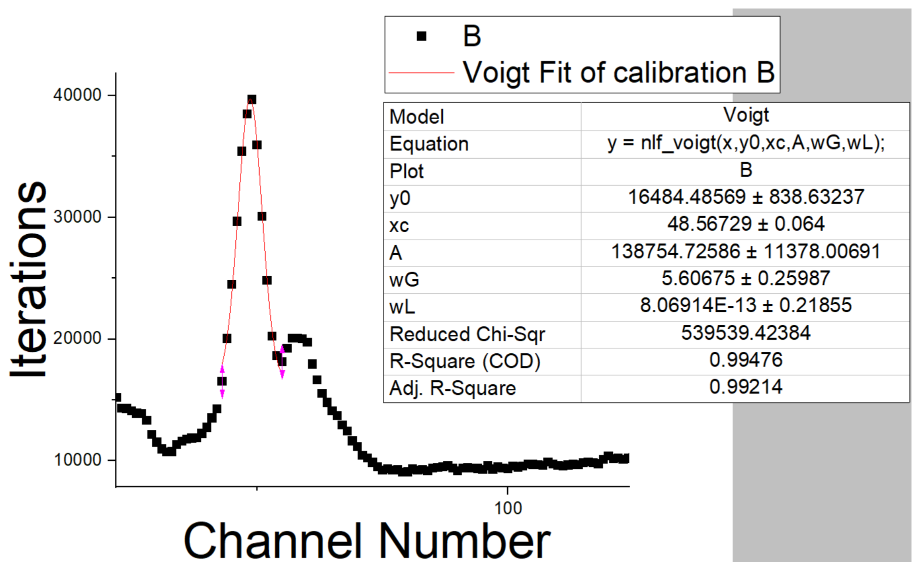

Figure (d): Voigt fit of Pb X-ray peak, corresponding to a channel number of 48.56729 ± 0.06400.

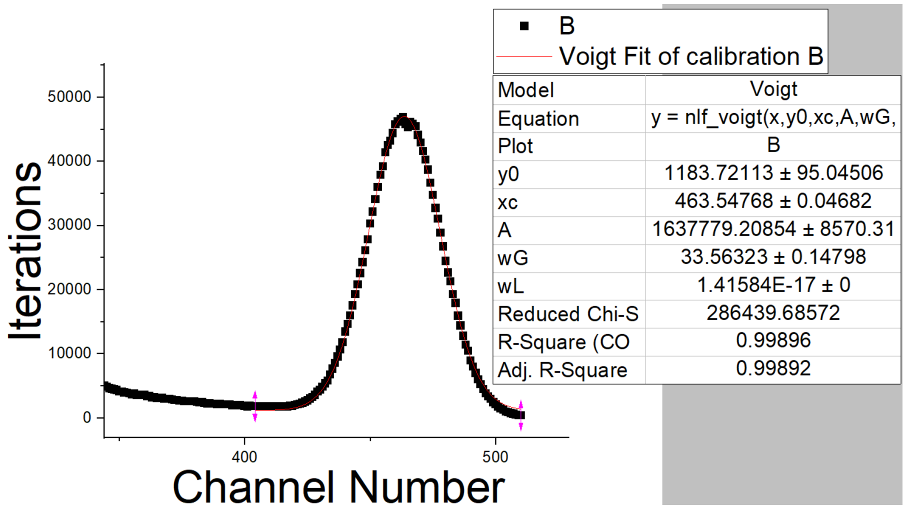

Figure (e): Voigt fit of Cs gamma peak, corresponding to a channel number of 463.54768 ± 0.04682.

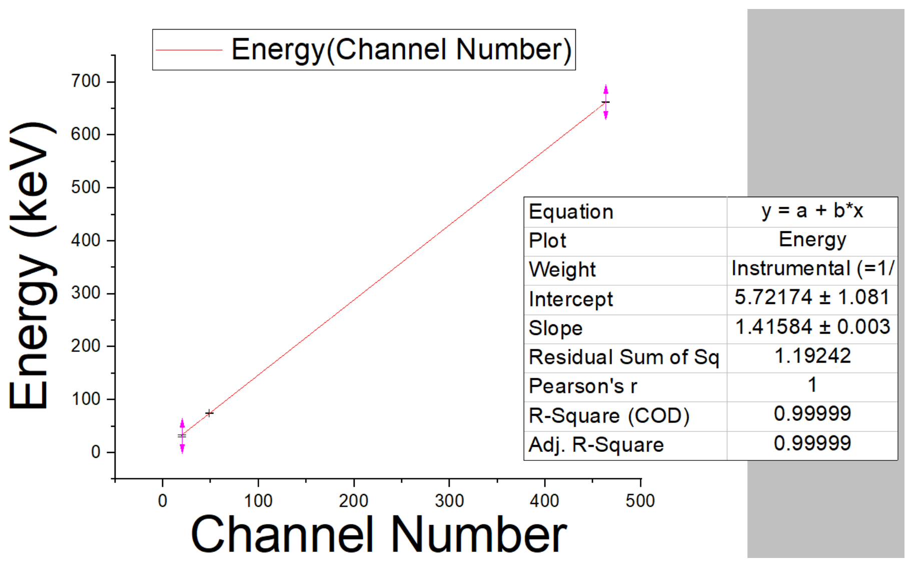

Figure (f): Calibration curve of energy and channel number. The corresponding equation
Energy $= (1.41584 \pm 0.00348) \times$ Channel Number $+ (5.72174 \pm 1.08138)$ was used to find values for energy from channel number for the remainder of the experiment.

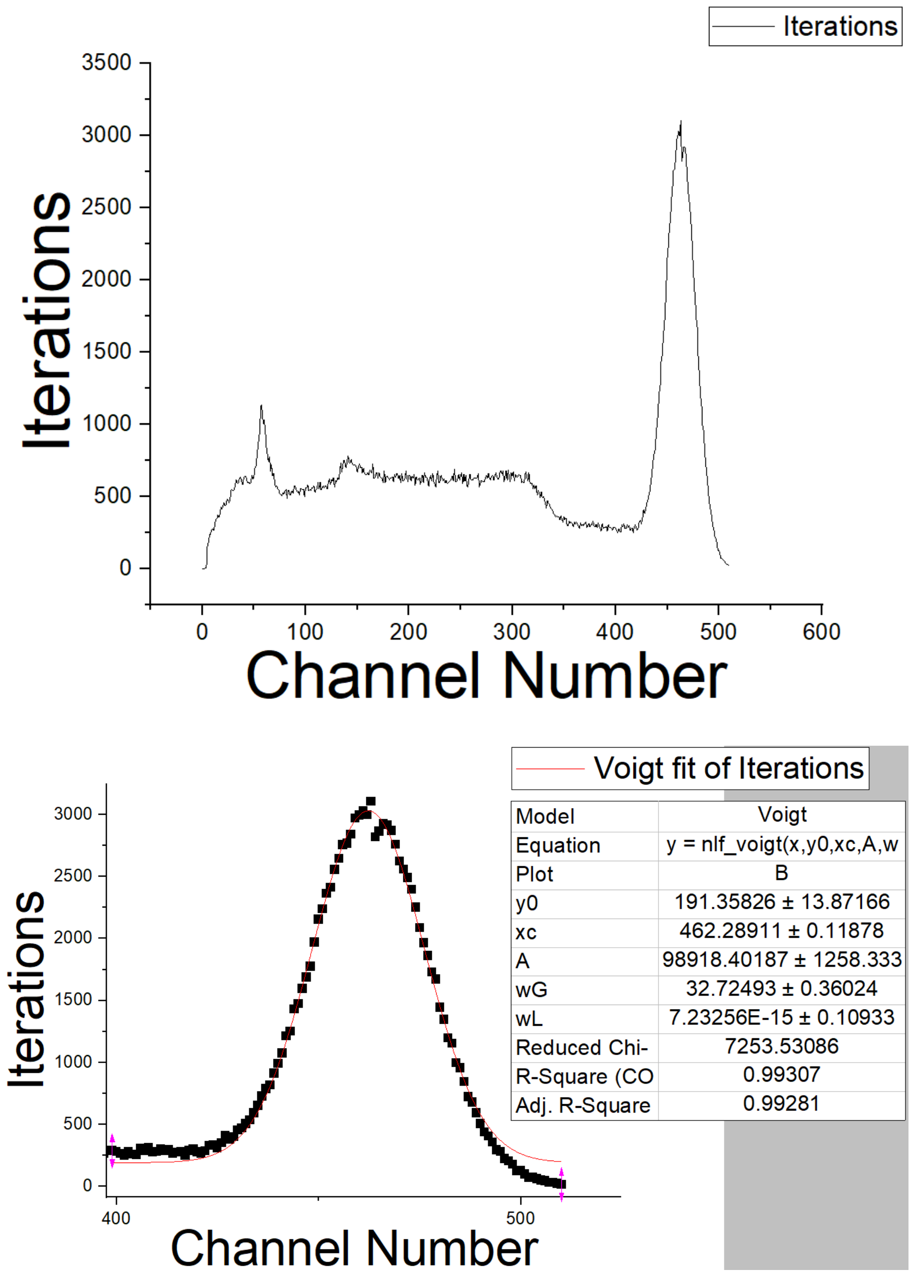

Figure (g): Energy spectrum for $\theta = 0$ and the corresponding peak location at channel number 462.28911 ± 0.11878. Data collected for 730 seconds.

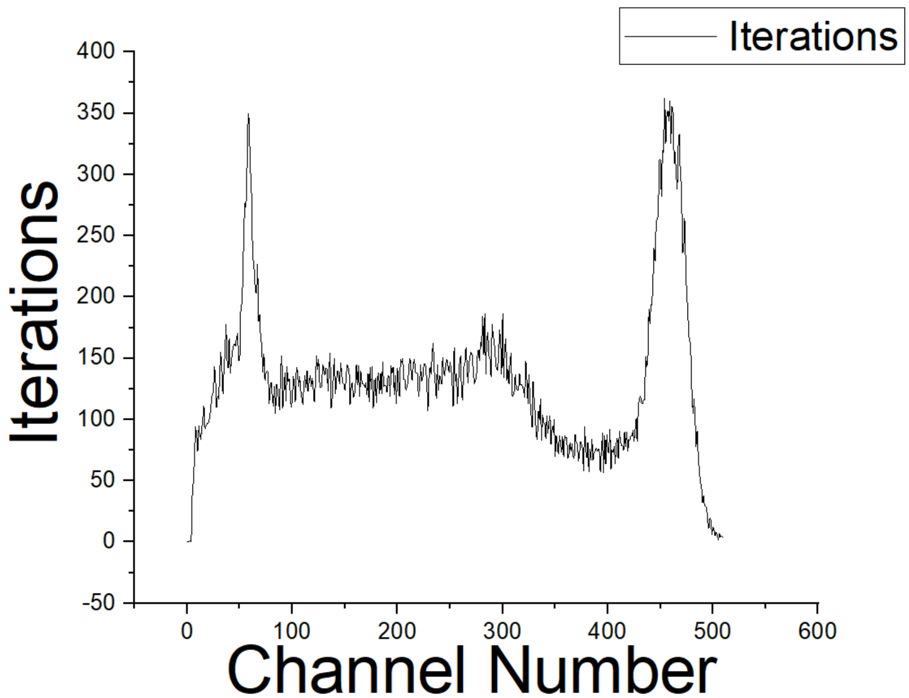

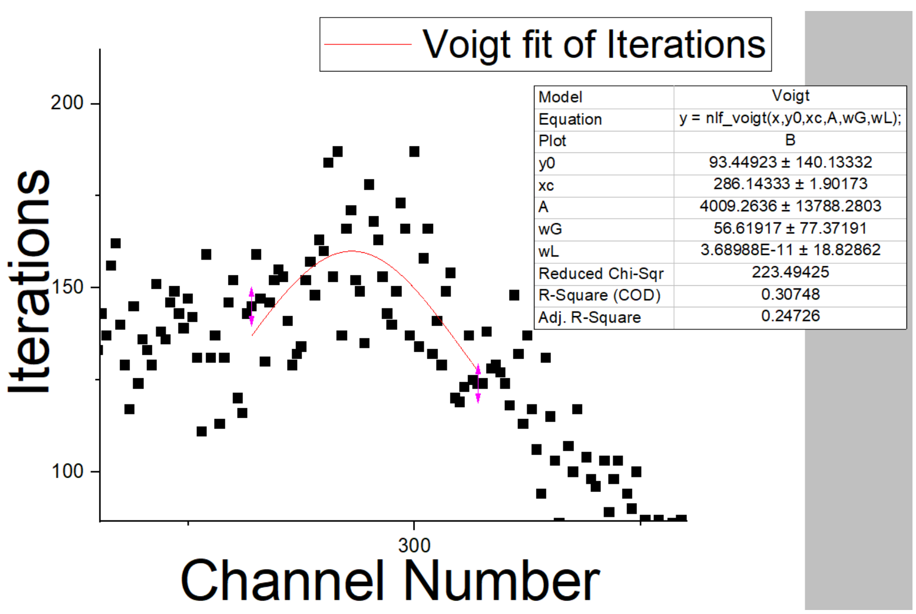

Figure (h): Energy spectrum for $\theta = \frac{\pi}{3}$ and the corresponding peak location at channel number 286.14333 ± 1.90173. Data collected for 964 seconds.

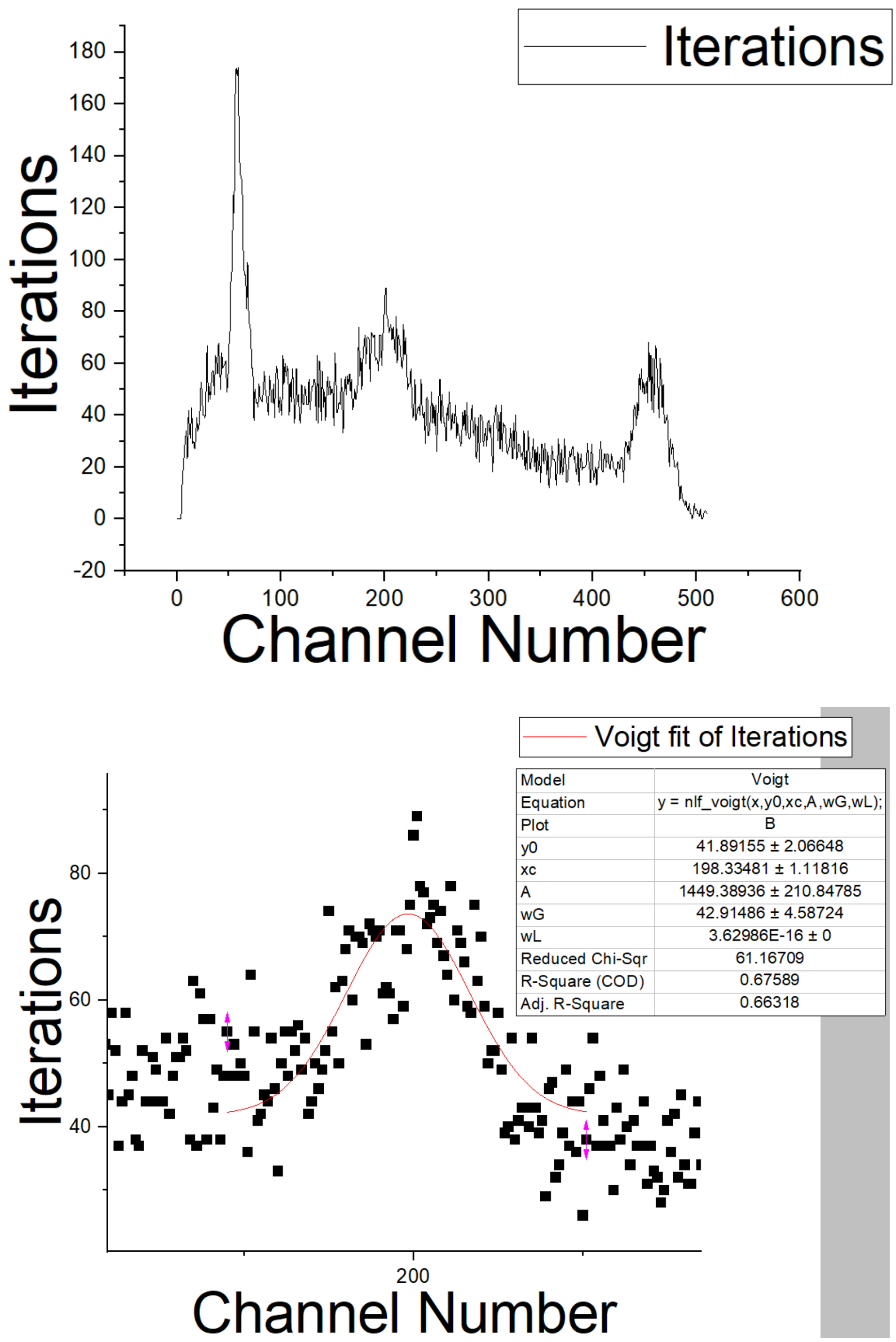

Figure (i): Energy spectrum for $\theta = \frac{\pi}{2}$ and the corresponding peak location at channel number 198.33481 ± 1.11816. Data collected for 853 seconds.

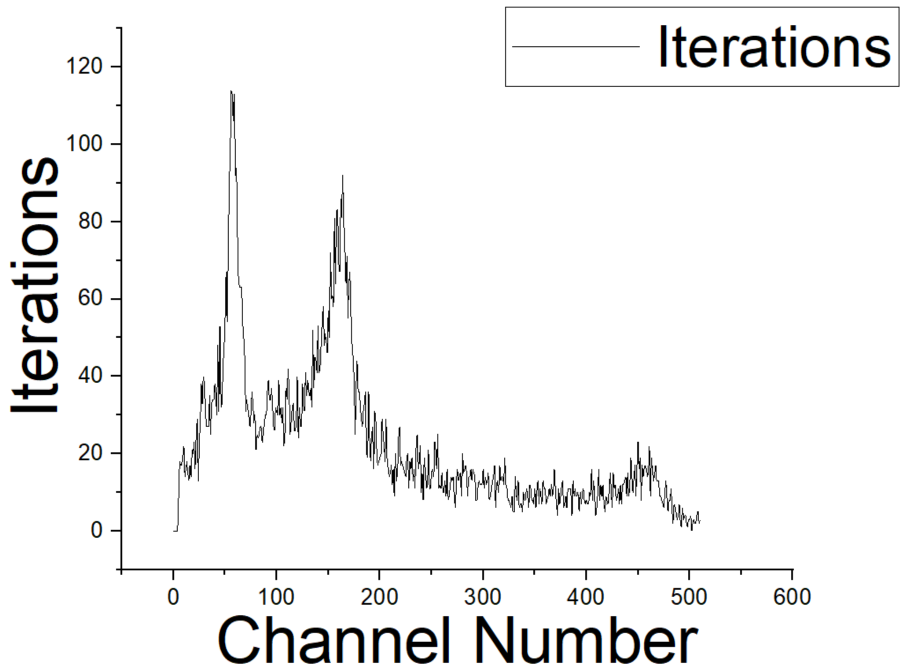

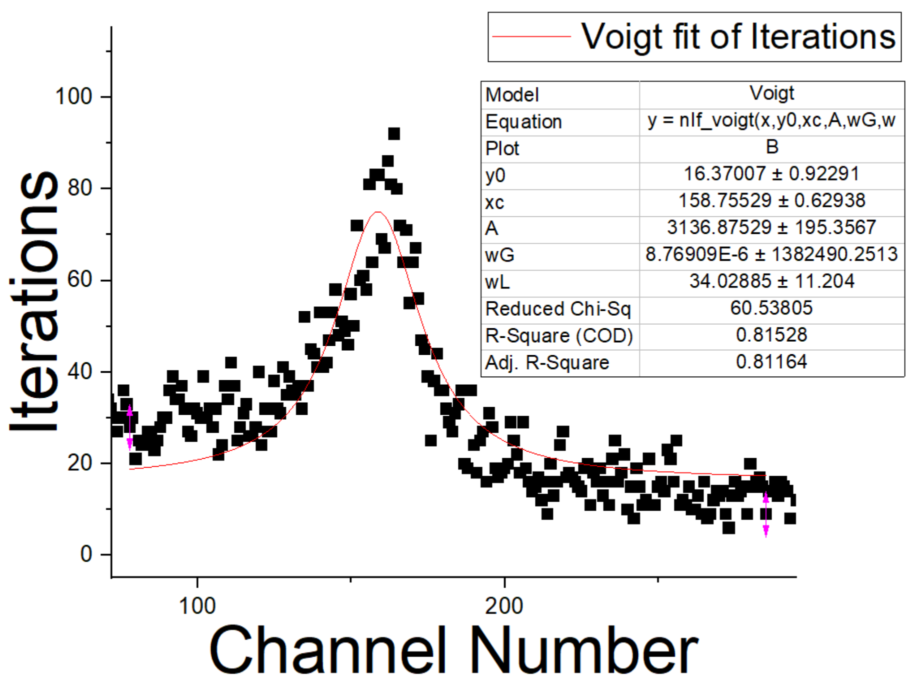

Figure (j): Energy spectrum for $\theta = \frac{2\pi}{3}$ and the corresponding peak location at channel number 158.75529 ± 0.62938. Data collected for 927 seconds.

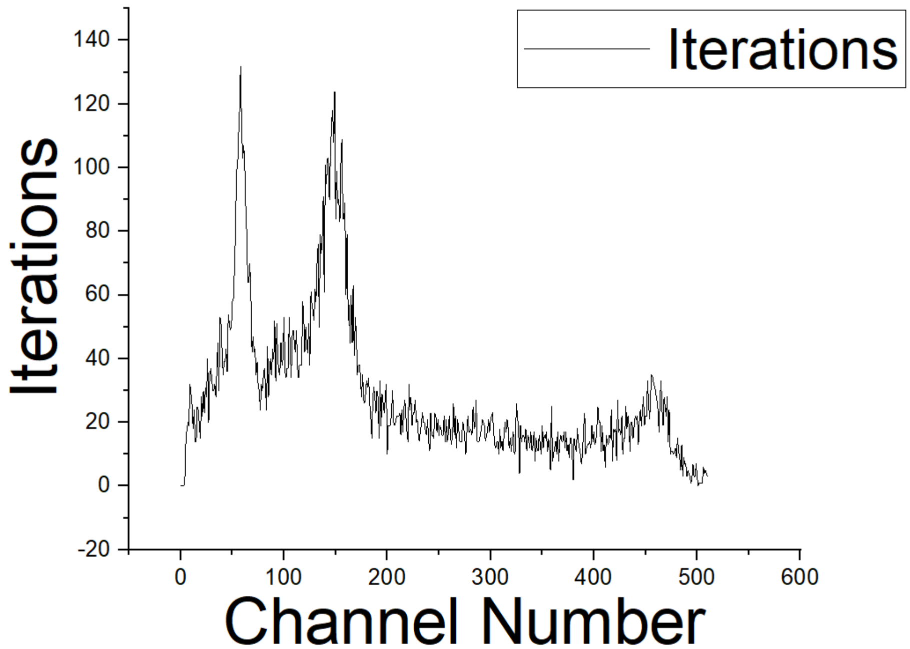

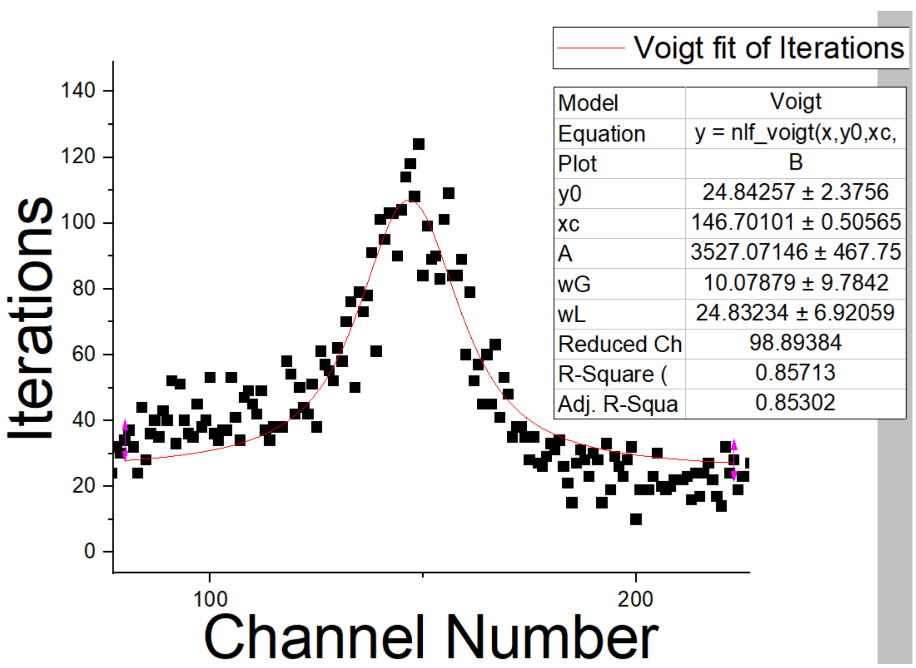

Figure (k): Energy spectrum for $\theta = \frac{3\pi}{4}$ and the corresponding peak location at channel number 146.70101 ± 0.50565. Data collected for 1,030 seconds.

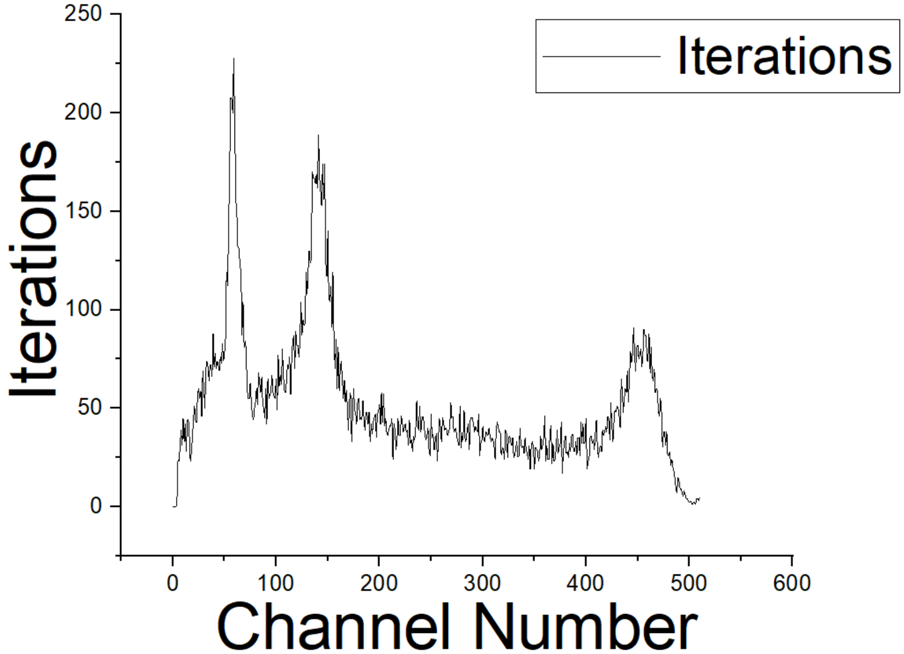

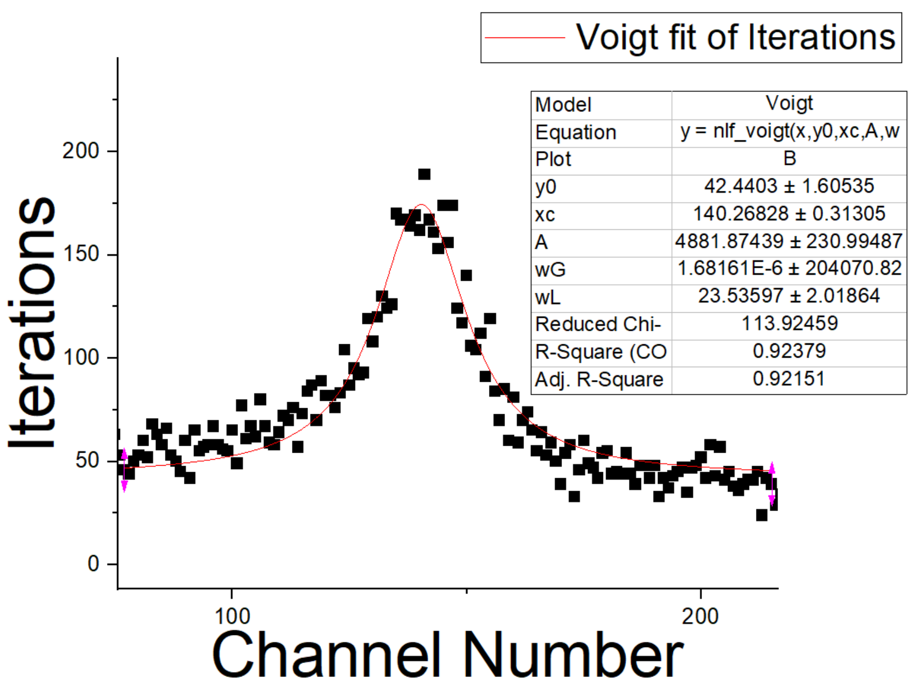

Figure (l): Energy spectrum for $\theta = \frac{5\pi}{6}$ and the corresponding peak location at channel number 140.26828 ± 0.31305. Data collected for 1,106 seconds.

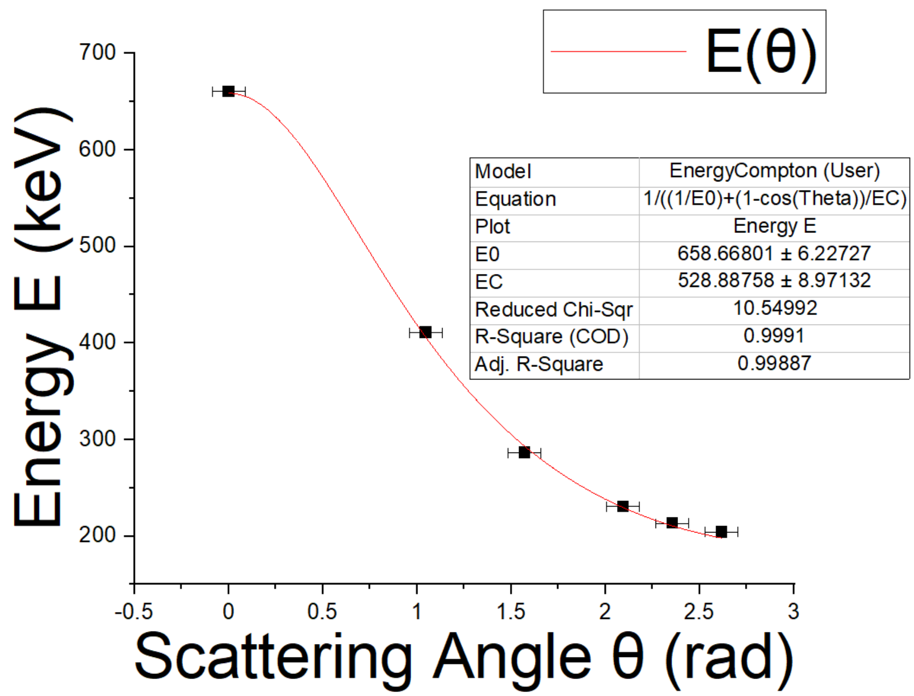

Figure (m): Plot of energy of scattered photon against scattering angle, fitted using equation (5). From this graph, the values for E_0 and E_C were estimated to be 658.66801 ± 6.22727 keV and 528.88758 ± 8.97132 keV, respectively.

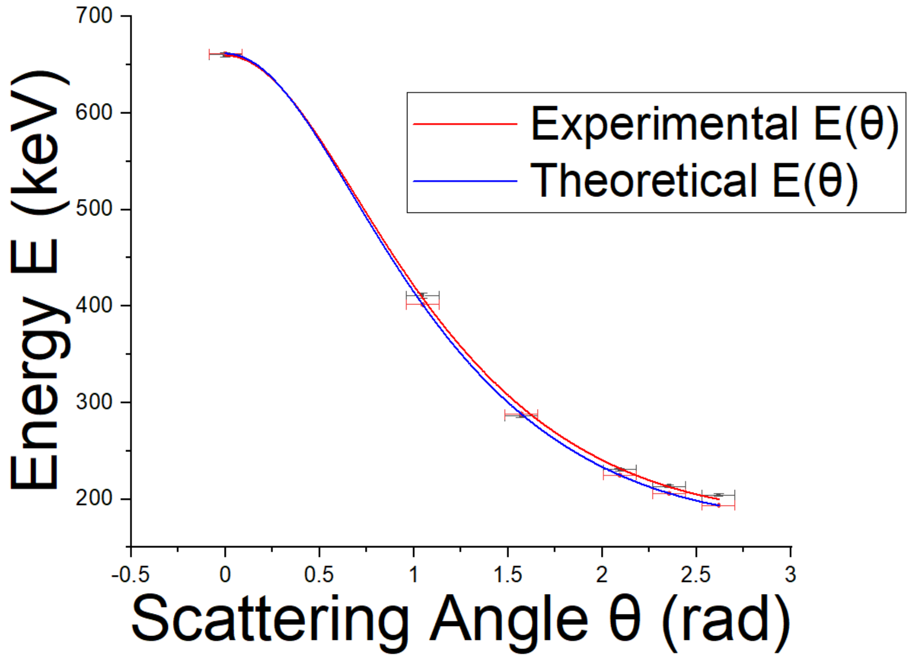

Figure (n): Comparison between experimental energy and theoretical energy of scattered photons.

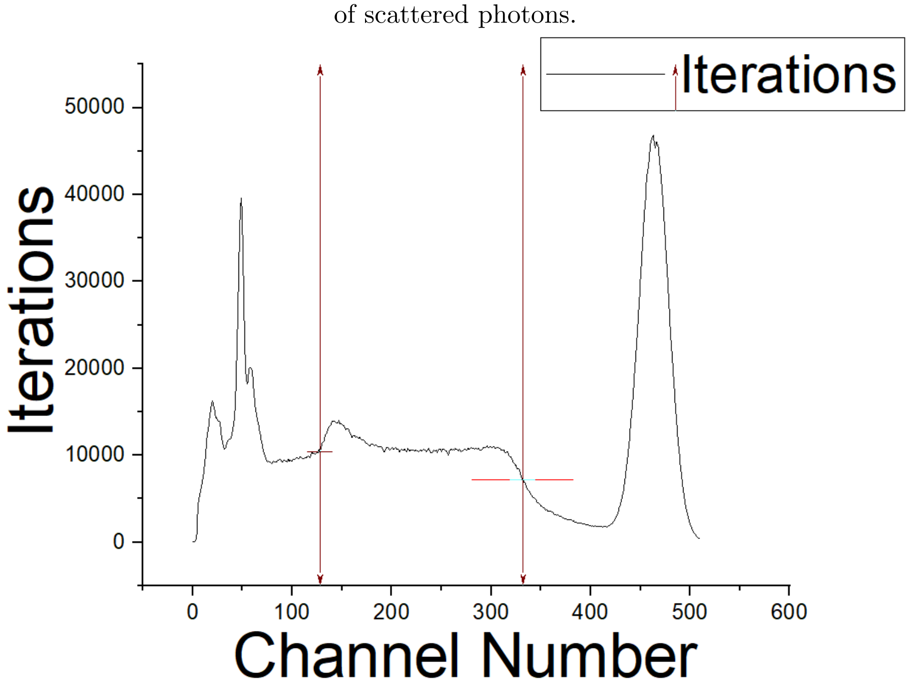

Figure (o): Estimates of the Compton edges. Channel numbers 128 and 332 correspond to 186.94926 ± 1.16953 keV and 475.78062 ± 1.58248 keV.

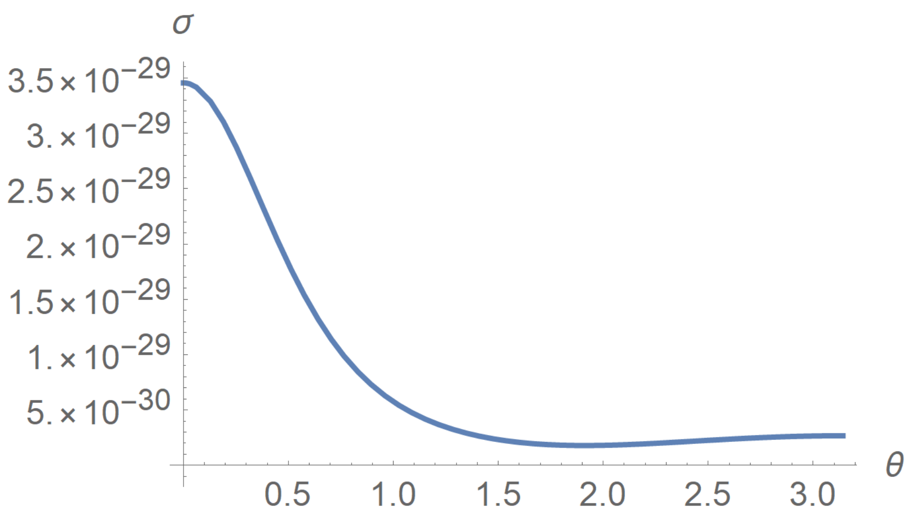

Figure (p): Plot of the dependence of the differential scattering cross section on the scattering angle for $E_0 = 661.657$ keV and $E_C = m_e^* c^2$.

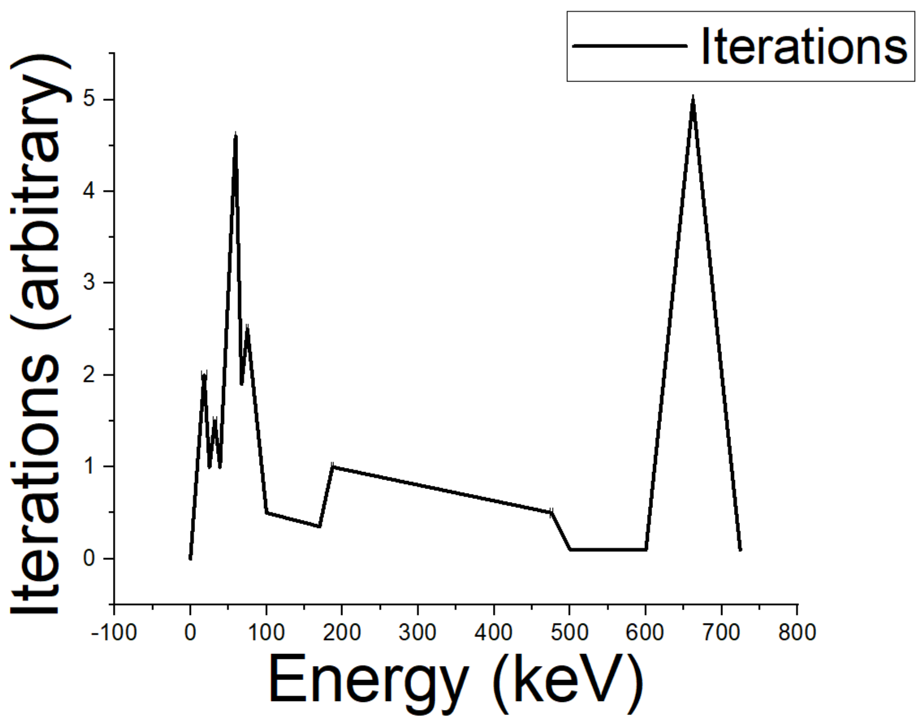

Figure (q): Rough simulation of energy spectra using experimental estimates.